

Report

**R-15-06**

December 2015



# Validating thermodynamic description of copper oxides and phosphates by controlled oxidation of OFP-copper

**Hans Magnusson**

**Fredrik Lindberg**

**Karin Frisk**

SVENSK KÄRNBRÄNSLEHANTERING AB

SWEDISH NUCLEAR FUEL  
AND WASTE MANAGEMENT CO

Box 250, SE-101 24 Stockholm  
Phone +46 8 459 84 00  
skb.se

SVENSK KÄRNBRÄNSLEHANTERING



ISSN 1402-3091

**SKB R-15-06**

ID 1494091

December 2015

# **Validating thermodynamic description of copper oxides and phosphates by controlled oxidation of OFP-copper**

Hans Magnusson, Fredrik Lindberg, Karin Frisk  
Swerea KIMAB AB

This report concerns a study which was conducted for Svensk Kärnbränslehantering AB (SKB). The conclusions and viewpoints presented in the report are those of the authors. SKB may draw modified conclusions, based on additional literature sources and/or expert opinions.

A pdf version of this document can be downloaded from [www.skb.se](http://www.skb.se).

© 2015 Svensk Kärnbränslehantering AB



## Abstract

Based on the thermodynamic evaluation of the Cu–H–O–S–P system made in a previous work, equilibrium calculations were made for oxygen-free phosphorus alloyed (OFP) copper. It was concluded that the most stable oxygen-compound for OFP copper should be copper phosphates rather than copper oxides. However, few direct experimental observations of phosphates in OFP-copper exist. For this reason, in the present work OFP-copper was oxidised at different conditions in order to validate the thermodynamic description and to experimentally show that copper phosphates are more stable than copper oxides at low partial pressure oxygen.

It is shown in this work that oxidising copper in inert gas with water vapour yields  $\text{Cu}_2\text{O}$  as the only surface copper oxide. With small additions of hydrogen to the gas, the surface copper oxides are no longer observed. These findings are in good agreement with thermodynamic calculations of copper oxide stability.

By oxidising at low partial pressure of oxygen it was experimentally shown how phosphorus rich oxides are present at lower partial pressure oxygen than copper oxides. This indicates a greater stability of phosphates compared to oxides, in agreement with thermodynamic calculations. The type of phosphate was studied with both SEM/EDS and TEM/EDS analysis. EDS analysis confirms that the phase is rich on phosphorus and oxygen. Electron diffraction shows best agreement to  $\text{Cu}_3(\text{PO}_4)_2$  copper phosphate.



# Contents

<b>1</b>	<b>Introduction</b>	7
<b>2</b>	<b>Materials and methods</b>	9
2.1	Materials	9
2.2	Oxidation	9
2.3	Characterisation	10
2.4	Thermodynamic calculations	10
<b>3</b>	<b>Determining suitable atmosphere for controlled oxidation of OFP-copper</b>	11
3.1	Oxidising, reducing and inert gases	11
3.2	Thermodynamic study of oxides	11
3.3	Stability of copper oxides in different gas mixtures	12
3.4	Oxidation parameters	13
<b>4</b>	<b>Characterisation of oxidised materials</b>	15
4.1	Oxidation and appearance	15
4.2	Oxidation 24 hours at 580 °C in N <sub>2</sub> /H <sub>2</sub> O atmosphere	17
4.3	Oxidation 24 hours at 600 °C in N <sub>2</sub> /H <sub>2</sub> O/H <sub>2</sub> atmosphere	18
<b>5</b>	<b>Discussion</b>	23
5.1	Surface copper oxides	23
5.2	Phosphorus rich oxides	24
<b>6</b>	<b>Conclusions</b>	27
	<b>References</b>	29





# 1 Introduction

Oxygen-free phosphorus copper (OFP-copper) is suggested as canister material for disposal of spent nuclear fuel in Sweden. Among the requirements on the copper canister material are a high creep ductility and resistance to corrosion (SKB 2010). The copper material is nearly pure copper with phosphorus as the only alloying element. The limits in composition are defined as phosphorus 30–100 ppm, sulphur less than 12 ppm, hydrogen less than 0.6 ppm, and oxygen less than some tens of ppm. The oxygen content in the copper ingots, in the initial material product, is specified to be below 5 ppm (SKB 2010). The low alloying contents makes it experimentally difficult to find and to characterise possible inclusions. With the help of thermodynamic calculations it is possible to determine where trace elements are distributed in the microstructure. The solubility of these elements in metallic copper, as well as the stability of possible inclusions including these trace elements can be determined.

Thermodynamic calculations are often used to determine the most stable set of phases at given conditions. The phases are normally crystalline phases but can also be liquids or gases. The conditions for the calculation are defined by the temperature, pressure and composition of the material or atmosphere. The thermodynamic equilibrium per definition describes the most stable set of phases. This is especially of interest in order to determine long-term stability of phases in OFP-Cu at low temperatures. It is also possible to derive the stability of metastable phases, and thereby discuss their possible significance in the application. In this work, focus is on the stability of copper phosphates in phosphorus alloyed copper material. Experiments suitable for thermodynamic characterisation are made and compared with calculations.

The accuracy of the calculations depends on the thermodynamic description of the alloying system that is being studied. The CALPHAD approach allows for a critical assessment of alloy systems based on experimental phase diagram and thermochemical information (Saunders and Miodownik 1998, Lukas et al. 2007). In a previous work, a thermodynamic evaluation for the alloying system Cu–H–O–S–P has been made (Magnusson and Frisk 2013, 2014). In the thermodynamic database two copper phosphates belonging to the CuO–P<sub>2</sub>O<sub>5</sub> system were included. These are the pyrophosphate Cu<sub>2</sub>P<sub>2</sub>O<sub>7</sub> and orthophosphate Cu<sub>3</sub>(PO<sub>4</sub>)<sub>2</sub>. The stability of these phosphates was derived based on reported enthalpy of formation found in literature. In an early study by Ball (1968) on the phase equilibrium in the CuO–P<sub>2</sub>O<sub>5</sub> system these phosphates were found stable at 900 °C, as well as an additional metaphosphate Cu(PO<sub>3</sub>)<sub>2</sub>. In addition, other copper phosphates have also been reported such as Cu<sub>5</sub>P<sub>2</sub>O<sub>10</sub>, Cu<sub>4</sub>(PO<sub>4</sub>)<sub>2</sub>O, CuPO<sub>3</sub> and Cu<sub>2</sub>PO<sub>4</sub> (Bamberger et al. 1997). The thermal stability of all these phosphates has been studied by Bamberger et al. (1997). It was concluded that the most stable phosphates were Cu<sub>2</sub>P<sub>2</sub>O<sub>7</sub> and Cu<sub>3</sub>(PO<sub>4</sub>)<sub>2</sub>.

Based on the thermodynamic description some calculations were made for OFP-copper (Magnusson and Frisk 2013, 2014). The equilibrium phases were copper sulphide Cu<sub>2</sub>S and copper phosphates. The sulphide is predicted to be stable from approximately 700 °C down to room temperature. Different copper phosphates are possible, depending on the hydrogen activity in copper and temperature; these are Cu<sub>2</sub>P<sub>2</sub>O<sub>7</sub>, Cu<sub>3</sub>(PO<sub>4</sub>)<sub>2</sub>, and Cu<sub>3</sub>(P<sub>2</sub>O<sub>6</sub>OH)<sub>2</sub>. Copper phosphates are stable from the copper melt down to room temperature. The presence of the copper sulphide has been experimentally verified for OFP-copper (Savolainen 2012). On the other hand, quite few experimental observations for copper phosphates in phosphorus alloyed copper material exist. An indirect observation of phosphorus-oxygen interaction in copper was made by Smart and Smith (1946). Conductivity measurements made for copper with low oxygen content showed a clear decrease in conductivity as a function of phosphorus additions. This is the expected behaviour of phosphorus additions in copper when all phosphorus is in solution. On the other hand, copper with high oxygen content did not show any significant loss in conductivity with phosphorus additions. This was believed to be due to the formation of phosphates which limited the phosphorus content in solution.

The aim with the present work is to experimentally validate some of the results from the previous thermodynamic evaluation made for the Cu–H–O–S–P system (Magnusson and Frisk 2013, 2014). Special interest is to verify that copper phosphates are more stable than copper oxides, since few observations of phosphates in phosphorus copper exist in literature. In the present work OFP-copper will be mildly oxidised. At oxidation the copper material is saturated with oxygen and a high phase fraction of phosphates or oxides is achieved. This will make it possible to find and characterise these oxides. By controlling the oxidising atmosphere a low oxygen potential can be chosen where copper phosphates, but not copper oxides, are stable. This will be a direct experimental validation that copper phosphates are more stable than copper oxides.

## 2 Materials and methods

### 2.1 Materials

Two different OFP-Cu materials have been used in this study. The main difference is the phosphorus content. A normal OFP-copper grade is taken from an extruded tube (SKB internal identity T48-R2), which contain 68 ppm phosphorus. The mean grain size was reported to be 60–240  $\mu\text{m}$ . The chemical composition is given in Table 2-1. A copper material with high phosphorus (106 ppm) OFP-Cu was taken from a study by Andersson et al. (1999). The copper material was extruded material provided by Outokumpu Poricopper OY, Finland. The grain size was reported to be 450  $\mu\text{m}$ . The chemical composition is given in Table 2-2.

**Table 2-1. The composition of the material designated normal phosphorus OFP-Cu. Values in wtppm.**

P	Ag	As	Bi	Cd	Fe	H	Mn	Ni	O	Pb
68.4	13.8	0.85	0.14	<0.003	1.06	0.37	<0.1	0.74	1.13	0.24
S	Sb	Se	Sn	Te	Zn					
4.77	0.072	0.22	0.084	0.063	<0.1					

**Table 2-2. The composition of the material designated high phosphorus OFP-Cu. Values in wtppm.**

P	H	O	S
106	<0.5	1.1	5

### 2.2 Oxidation

Small cylindrical copper specimens were used for oxidation, approximately 10 mm in diameter and 4 mm in thickness. Oxidation was performed by exposing the copper materials to selected atmospheres. The different copper grades were oxidised simultaneously. A schematic image of the experimental setup is shown in Figure 2-1. The oxidation was made in an air-tight alumina tube furnace. The setup allows for mixing both the  $\text{N}_2/\text{H}_2$  gas ratio and the ratio dry/moisturised gas. The mixed gases enter the air-tight tube which is heated by the tube furnace to selected temperature. The material oxidise at the chosen temperature and atmosphere. The moisture content was logged by a dew-point meter. AGA instrument nitrogen grade 5.0 was used, which specifies the purity of the gas to 99.999 % and impurities ( $\text{H}_2\text{O}$ ,  $\text{O}_2$ ,  $\text{C}_n\text{H}_m$ ) are at ppm level. AGA instrument hydrogen grade 4.5 was used, giving 99.995 % purity of hydrogen gas with less than 5 ppm  $\text{O}_2$  and  $\text{H}_2\text{O}$ .

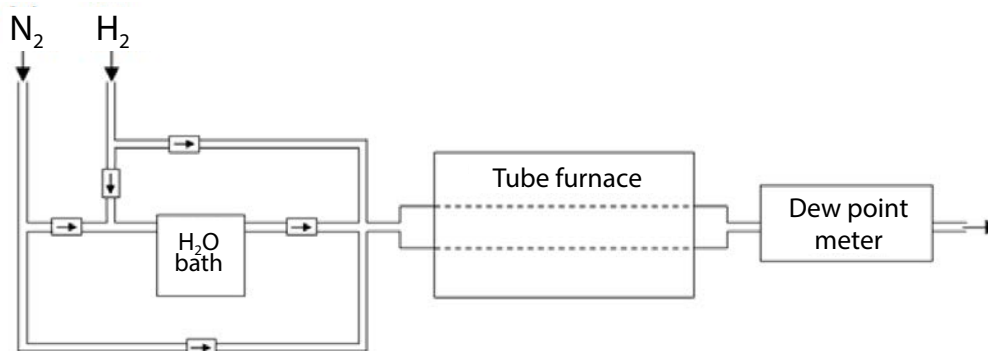


**Figure 2-1.** Experimental setup of oxidation showing how different gases can be mixed, and enters the air-tight tube furnace with copper samples. The moisture content is measured by dew-point meter.

## 2.3 Characterisation

Microstructural characterisation was made using JEOL JSM-7100F scanning electron microscope (SEM) with energy-dispersive X-ray spectroscopy (EDS) from Oxford instruments for element characterisation. Imaging and analysis were done at 20 and 5 kV. The surface of the oxidised sample was analysed. In addition, cross-sectional images of the oxidised surface were produced by adjoining two of these sample surfaces face-to-face and then grind and polish down to 4 000 grip SiC paper. Further work has also been made using a JEOL JEM-2100F transmission electron microscope (TEM). Chemical analysis was made using INCA X-sight EDS detector. The analysed sample was prepared by ion milling using a SEM FEI Quanta 3D equipped with focused ion beam (FIB).

## 2.4 Thermodynamic calculations

Thermodynamic calculations in this work were made using the Thermo-Calc software (Thermo-Calc 2015). The thermodynamic calculations for copper material were made using the database evaluated for the Cu–H–O–S–P system in a previous work (Magnusson and Frisk 2013, 2014). This thermodynamic database included the gas phase but not nitrogen gas which is used as carrier gas at oxidation in this work. For this reason, some complementary calculations were made for the gas phase using the Scientific Group Thermodata (SGTE) substance database SSUB3 (SSUB3, 2015).

## 3 Determining suitable atmosphere for controlled oxidation of OFP-copper

### 3.1 Oxidising, reducing and inert gases

In this chapter suitable oxidising atmospheres will be calculated. The aim is to find an atmosphere that is sufficiently oxidising to produce copper phosphates, but reducing enough not to form copper oxides.

Different gas mixtures can be used in order to reach the desired oxidising potential. In general, different gases can be characterised according to their different properties, such as oxidising gases, reducing gases, and inert gases. Some examples are:

- Oxidising gases: oxygen gas  $O_2$ , or other gases that decompose into high content free oxygen such as  $N_2O$ , or low content free oxygen such as  $CO_2$  and  $H_2O$ .
- Reducing gases: hydrogen  $H_2$ , or gases that decompose to hydrogen such as  $NH_3$ ,  $CH_4$ , or  $CH_3OH$ . It can also be gases that have a high affinity to oxygen, such as  $CO$ .
- Inert gases: nitrogen  $N_2$  or argon  $Ar$ .

An atmosphere including free oxygen ( $O_2$ ) will have a high oxidising potential. The oxidising potential will fall by dilution with inert nitrogen or argon gases. The aimed oxidising potential in this work is very low, and it is difficult to reach this oxygen potential based on an atmosphere with oxygen  $O_2$  as in-going gas. A better approach is to substitute oxygen gas with a mild oxidant, such as  $H_2O$  or  $CO_2$ . These gases are considered as mild oxidants since only a minor fraction of the water vapour will decompose into oxygen and hydrogen. This water reaction directly offers low oxygen partial pressure. To further lower the oxidising potential this water vapour can be mixed with an inert gas or an additional reducing gas. For instance, if hydrogen is added it will react with the low content of free oxygen and the oxidising potential will be low.

### 3.2 Thermodynamic study of oxides

The high reactivity between oxygen and metallic elements make equilibrium studies of oxides difficult. With a high reactivity an oxide can form early in a metallurgical process and then remain to low-temperature service. If that oxide is not the equilibrium oxide it will require long-range diffusion in the metallic material in order to reach the equilibrium phase. This process depends on both the diffusivity and solubility. The strongest limitation for this reaction in the present work is the extremely low solubility of oxygen in copper. Instead of equilibrium studies in solid material, surface reactions can be evaluated. Surface reactions allow for short-range diffusion which decreases the reaction time and equilibrium between the material and the gas is quickly reached. By exposing the copper material to a carefully chosen oxidising atmosphere the stability of oxides and phosphates can be evaluated.

The copper phosphates are believed to be more stable than copper oxides. An oxidising atmosphere should be chosen that corresponds to a low oxidising potential were copper oxides are not predicted to be stable but copper phosphates are. Oxidising at higher partial pressure oxygen is also of interest, but then the copper phosphates are expected to be found in a dense oxide layer of  $CuO/Cu_2O$  oxides. The phase fraction of phosphates will be minor since OFP-copper has typically a low content of phosphorus, below 100 ppm. This gives a maximum phase fraction of 0.1 % if the material is saturated with oxygen and all phosphorus have reacted. A similar experimental approach to oxidise steels containing even stronger oxide formers, such as chromium, manganese and silicon, has previously been made (Magnusson et al. 2013). Low alloyed steels were oxidised at low partial pressure at 800–1 000 °C. Internal oxides were found up to 50  $\mu m$  into the material. This approach will now be applied for OFP-copper.

### 3.3 Stability of copper oxides in different gas mixtures

The stability of copper oxides  $\text{CuO}$  and  $\text{Cu}_2\text{O}$ , and metallic copper (denoted FCC\_A1) is presented in Figure 3-1, as a function of oxygen activity and temperature. In this figure the stability of copper phosphates  $\text{Cu}_2\text{P}_2\text{O}_7$  and  $\text{Cu}_3(\text{PO}_4)_2$  are shown as well. The oxygen activity refers to the oxygen content in the copper material relative the oxygen content in copper when in equilibrium with 1 atmosphere pure oxygen gas. The concept of activities allows for comparing different oxygen equilibria, and the term activity can be seen as an effective concentration for the system. At equilibrium the activity is the same in all present phases such as the copper material, oxides, and gas phase. This definition makes it possible to compare the oxygen activity in the copper material with the oxygen activity in the gas. For the gas phase the partial pressure oxygen can be estimated as the square root of the oxygen activity, according to Sievert's law.

Calculations for the solid material and oxides are made using the thermodynamic database by Magnusson and Frisk (2013, 2014). The figure shows that at low oxygen activities and high temperatures no oxides are stable and only metallic FCC\_A1 is present. To the right in the figure the oxygen activity increases forming first copper phosphates  $\text{Cu}_3(\text{PO}_4)_2$  (denoted  $\text{Cu}_3\text{P}_2\text{O}_8$ ) or  $\text{Cu}_2\text{P}_2\text{O}_7$ . These phosphates are stable in a metal copper matrix at these oxygen activities. With increasing activity the metal matrix oxidises and the most stable copper oxide,  $\text{Cu}_2\text{O}$ , forms first. At even higher partial pressure oxygen the other copper oxide,  $\text{CuO}$ , is stable as well.

Figure 3-1 also shows the oxidising activity for different gas mixtures:  $\text{N}_2+1\%\text{H}_2\text{O}$  and  $\text{N}_2+1\%\text{H}_2\text{O}+0.01\%\text{H}_2$ . The oxygen activity for these gas mixtures are calculated using SSUB3 thermodynamic database (SSUB3 2015). The gas mixture with a mild oxidant,  $\text{N}_2+1\%\text{H}_2\text{O}$ , yields copper phosphates in a copper oxide  $\text{Cu}_2\text{O}$ . In order to get a surface without copper oxides but with copper phosphates, a gas mixture with both water vapour and hydrogen can be used, like  $\text{N}_2+1\%\text{H}_2\text{O}+0.01\%\text{H}_2$ . By oxidising at the oxygen activities obtained in this gas it can be experimentally shown if copper phosphates are more stable than copper oxides.

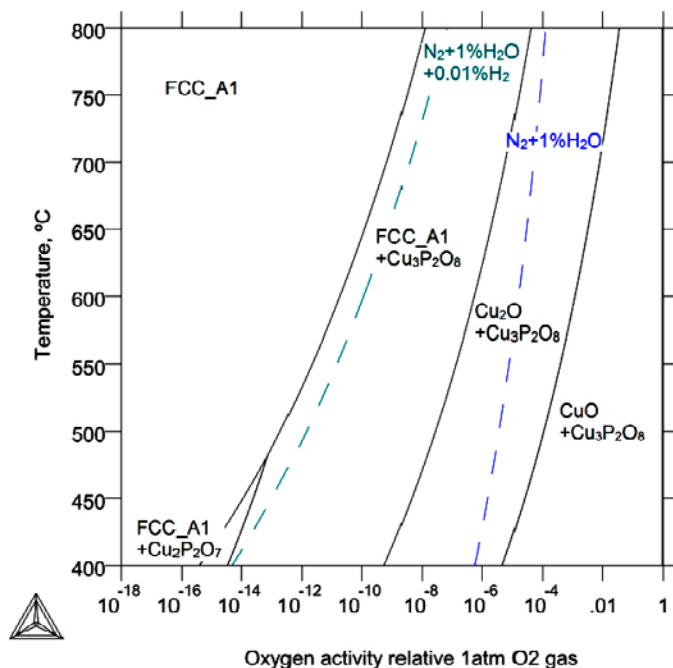


**Figure 3-1.** Stable phases as functions of temperature and oxygen activity. As comparison, the oxygen activities in different gas mixture are shown as well.

### 3.4 Oxidation parameters

Oxidation with two different atmospheres was made in this study, as summarised in Table 3-1. A N<sub>2</sub>/H<sub>2</sub>O/H<sub>2</sub> atmosphere was chosen in order to produce an atmosphere with sufficiently low partial pressure oxygen so that only copper phosphates are stable but no copper oxides. The atmosphere was achieved by bubbling nitrogen gas with a flux of 1 l/min through water. The dew-point was measured to approximately 24 °C. Minor content of hydrogen gas (3.2 ml/min) was added to this atmosphere. The calculated oxygen activity and partial pressure is given in Table 3-1. An additional oxidation was made without any added hydrogen gas. This type of experiments yields much higher partial pressure oxygen.

**Table 3-1. The oxidising conditions used in this study, together with the calculated oxygen activities.**

Temperature	Time	Oxidation atmosphere	Oxygen activity relative 1 atm O <sub>2</sub> gas	Oxygen partial pressure, atm
580 °C	24 h	N <sub>2</sub> + 2.9 % H <sub>2</sub> O	$2 \times 10^{-5}$	$4 \times 10^{-10}$
600 °C	24 h	N <sub>2</sub> + 2.9 % H <sub>2</sub> O + 0.32 % H <sub>2</sub>	$1 \times 10^{-11}$	$1 \times 10^{-22}$





## 4 Characterisation of oxidised materials

### 4.1 Oxidation and appearance

The oxidised copper samples are shown in Figure 4-1. The material oxidised at 580 °C in  $N_2/H_2O$  atmosphere gave an oxidised brown surface. The oxide layer had a weak adhesion to the copper substrate. The material oxidised at 600 °C  $N_2/H_2O/H_2$  sample did not show this brown oxide layer. This sample appears metallic but with a matte surface when comparing with the shiny non-oxidised copper.

The surfaces of these samples were investigated with SEM and EDS characterisation. The surfaces of two oxidised normal OFP-copper materials were adjoined face-to-face, grinded and polished in order to study cross-sectional images. This is shown in Figure 4-2. The upper part shows the 580 °C  $N_2/H_2O$  sample which has a continuous oxide layer on the surface appearing darker grey. The composition of the oxide layer was investigated with EDS, which gave 70.6Cu–29.6O in atomic percent. This is close to  $Cu_2O$  stoichiometry. The thickness of the oxide layer is 1–5  $\mu m$ . The lower part of the image is the 600 °C  $N_2/H_2O/H_2$  sample. This material did not produce any continuous oxide layer, which explains why the material appears metallic in Figure 4-1.

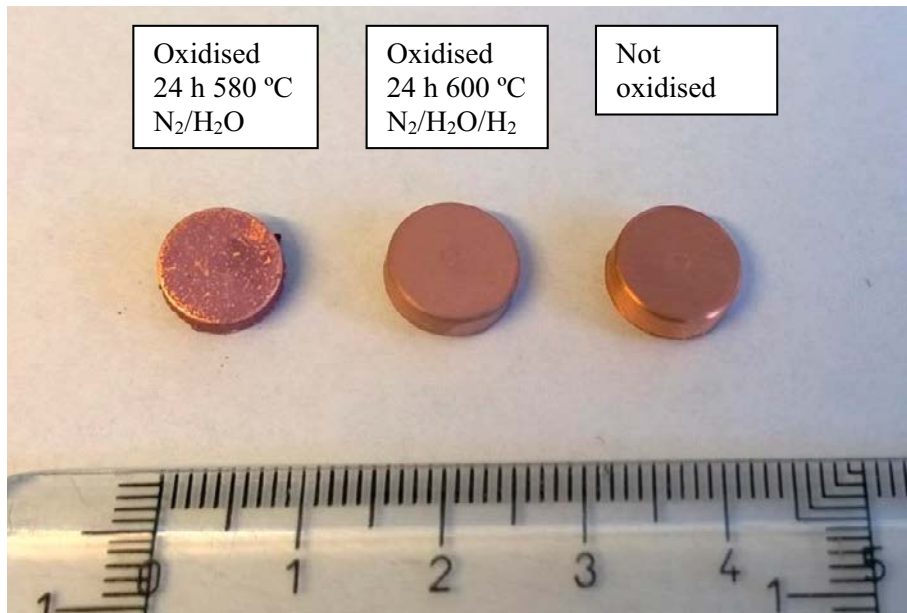


**Figure 4-1.** Oxidised samples compared to unaffected metallic copper.

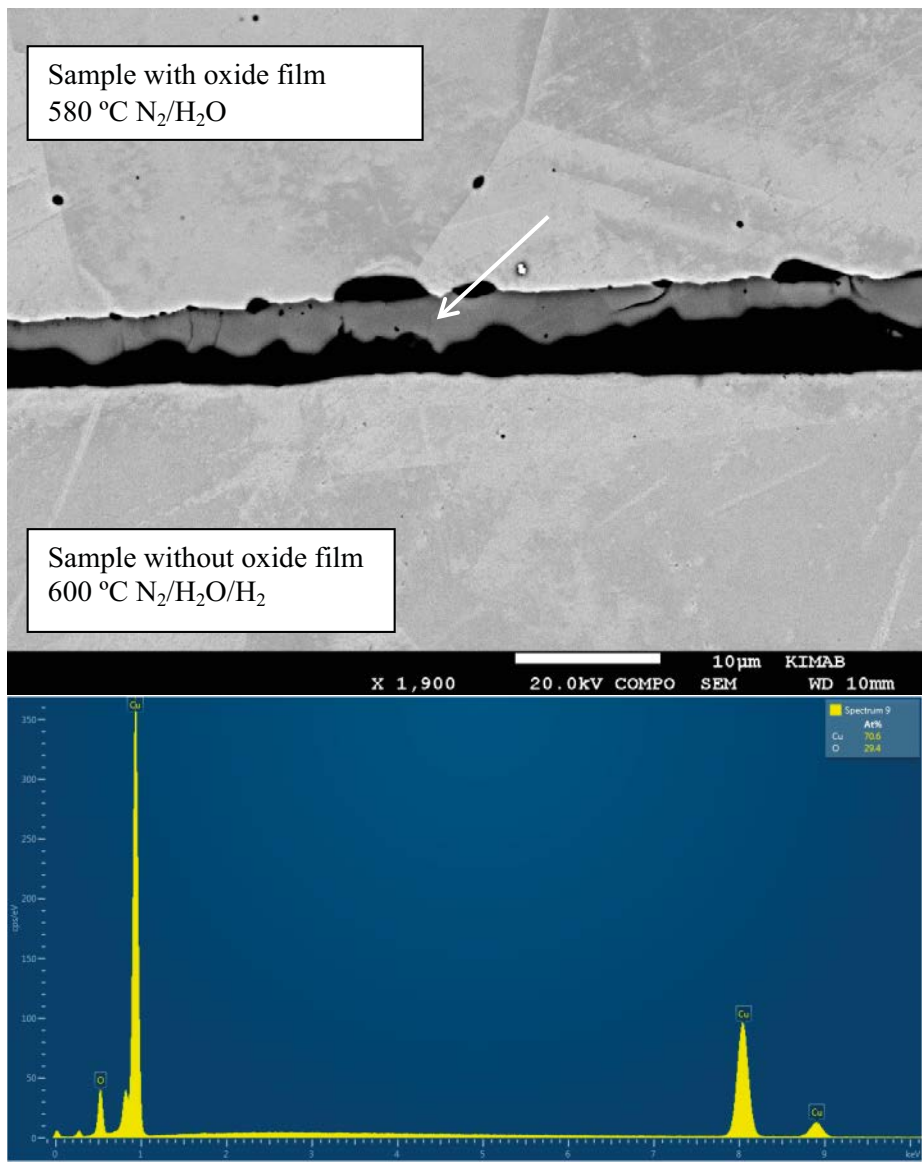


**Figure 4-2.** Cross-sectional images of oxidised normal OFP-Cu. Upper part shows copper with thin oxide layer (Cu<sub>2</sub>O). The lower part was oxidised at lower partial pressure oxygen and do not show any copper oxide film. The lower image is the EDS analysis of the copper oxide that is indicated by the arrow in the upper figure. The analysis is 70.6Cu–29.4O in atomic percent.

## 4.2 Oxidation 24 hours at 580 °C in N<sub>2</sub>/H<sub>2</sub>O atmosphere

Tiny particulates were found in the Cu<sub>2</sub>O oxide film. This is shown in Figure 4-3, where dark grey particulates of less than 200 nm in size are present. Due to the small size it was not possible to get a good chemical analysis of it. The electron beam has an interaction volume that is larger than the particulate size, and the analysis gives a mixed spectrum of both Cu<sub>2</sub>O oxide and a phosphorus-rich oxide. EDS analysis indicates an increasing phosphorus content when including the particulate, compared to only Cu<sub>2</sub>O oxide.

An additional measurement of these small oxides is shown in Figure 4-4. The EDS analysis with mixed spectrum gave 60.6Cu–35.2O–4.1P. Compared to the stoichiometric Cu<sub>2</sub>O oxide the phosphorus and oxygen contents have increased, which again suggests the presence of copper phosphates. Both phosphates Cu<sub>2</sub>P<sub>2</sub>O<sub>7</sub> and Cu<sub>3</sub>(PO<sub>4</sub>)<sub>2</sub> have higher oxygen contents than Cu<sub>2</sub>O.

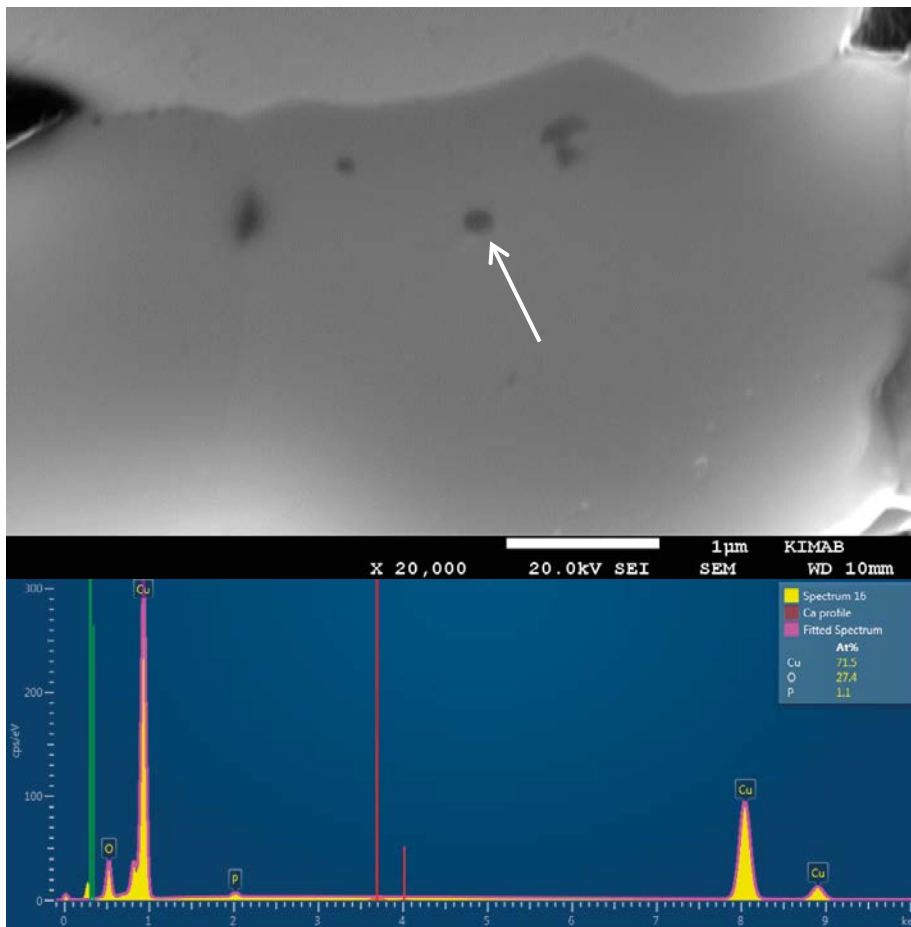


**Figure 4-3.** SEM image of oxidised normal OFP-Cu at 580 °C in N<sub>2</sub>/H<sub>2</sub>O atmosphere. The image shows upper part unaffected copper, lower part oxidised layer (Cu<sub>2</sub>O) with small particulates rich on phosphorus. The phosphorus containing oxides are indicated by the arrow in micrograph, and its analysis results are shown as well.

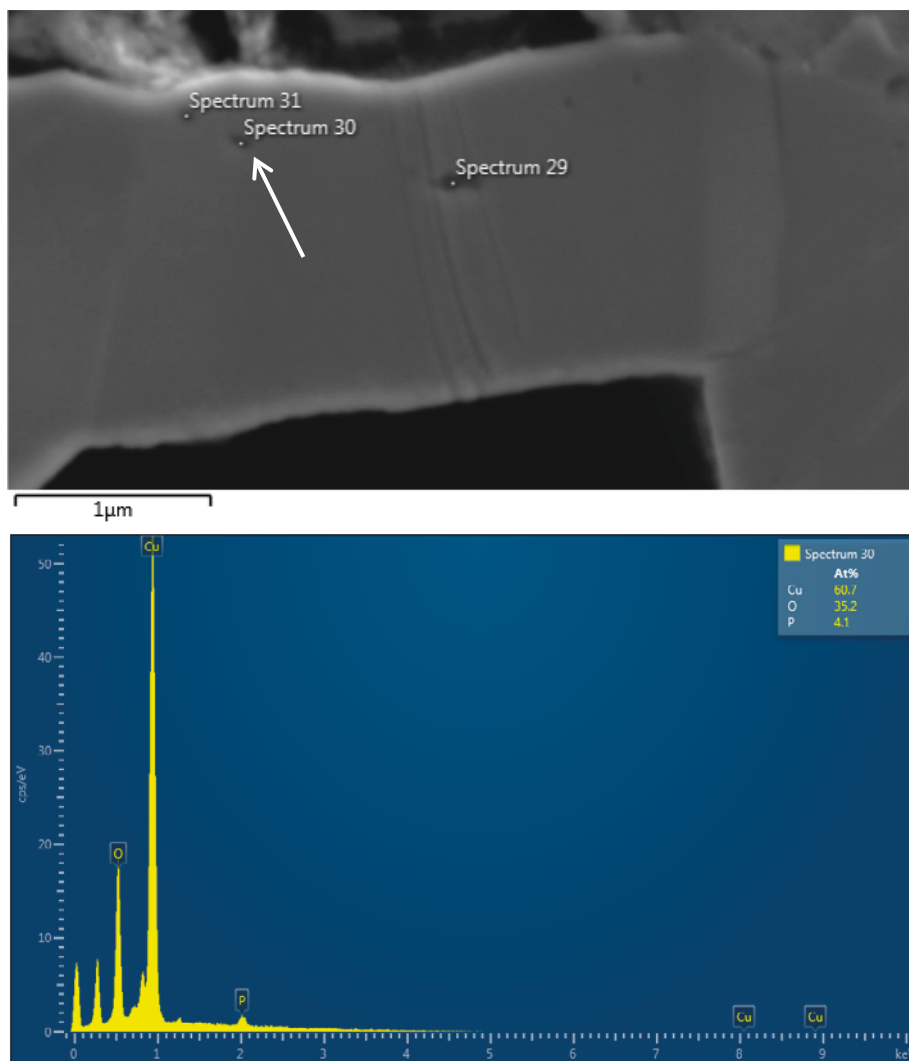


**Figure 4-4.** SEM image of oxidised normal OFP-Cu at 580 °C in  $N_2/H_2O$  atmosphere. The chemical analysis gives 60.7Cu–35.2O–4.1P.

### 4.3 Oxidation 24 hours at 600 °C in $N_2/H_2O/H_2$ atmosphere

The normal phosphorus OFP copper oxidised at 600 °C in  $N_2/H_2O/H_2$  gas did not give any copper based surface oxides, as shown previously in Figure 4-2. However, phosphorus rich oxides were found on the surface of the sample. The low fraction of phosphorus oxides can be explained by the low phosphorus content of the material (68 ppm). An example of a phosphorus rich oxide on the surface is shown in Figure 4-5. The EDS measurements give 56.7Cu–14.8O–5.6P. A significant amount of carbon is also present, which is probably due to contamination from the atmosphere. This oxide is on a metallic copper surface, which will give a mixed spectrum of phosphorus oxide plus metallic copper. For this reason, the oxygen content is much lower than in previous measurements and the copper content is quite high.

Additional measurements of the high phosphorus OFP-copper is shown in Figure 4-6. The surface of the oxidised sample and the corresponding Cu, O, S, and P element maps are shown. The grain structure is pronounced by the oxidising, and inclusions such as oxides and sulphides can be found in the grain boundaries. This indicates that the mild oxidation was successful. Overlap between phosphorus and oxygen are seen. It can also be seen that some more oxygen marks are present, which could be due to the oxidation of other trace elements in copper that are strong oxide formers like silicon, aluminium, manganese etc. EDS measurement of a phosphorus rich oxide, which is indicated in the figure, has composition 51.2Cu–37.2O–6.6P in atomic composition.

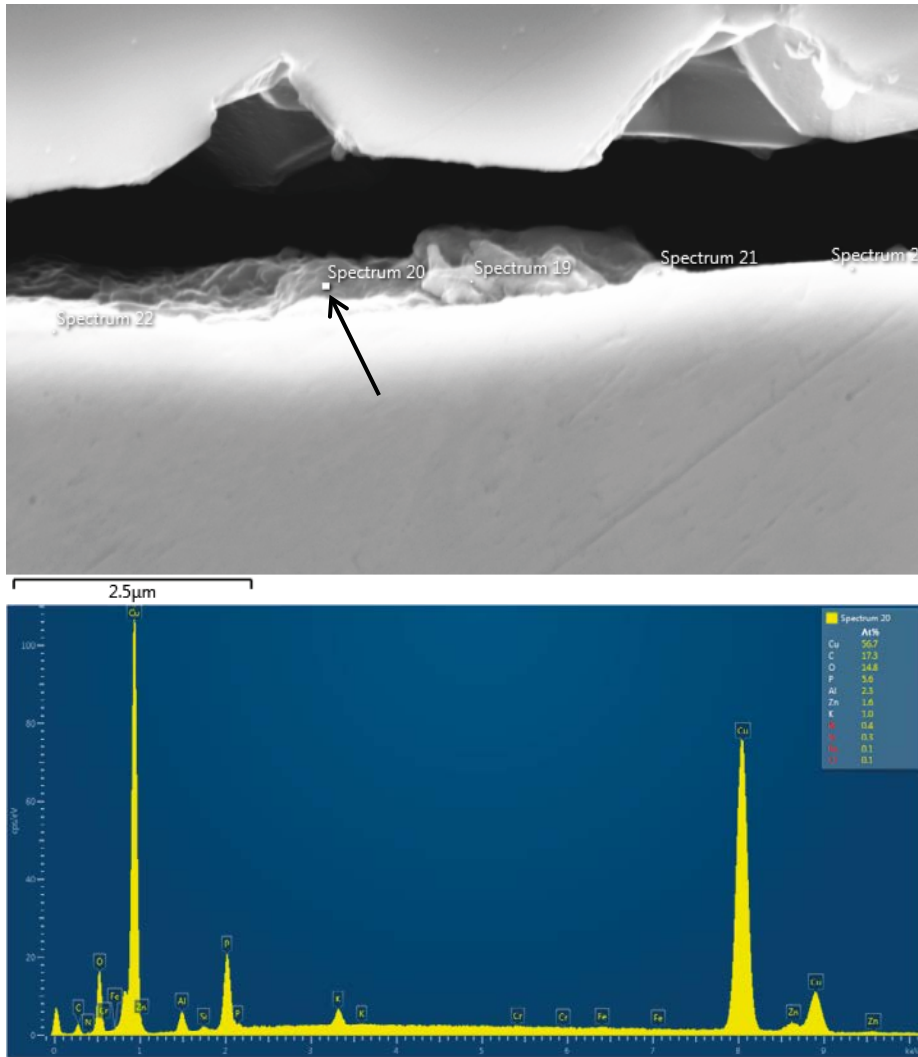


**Figure 4-5.** Spectrum 20 (black arrow) is a phosphorus rich oxide on the surface of oxidised normal OFP-Cu at 600 °C in  $N_2/H_2O/H_2$ . EDS measurement gives 56.7Cu–14.8O–5.6P. The measurement gives also other elements such as carbon (17.3 %), but this is most likely contamination.

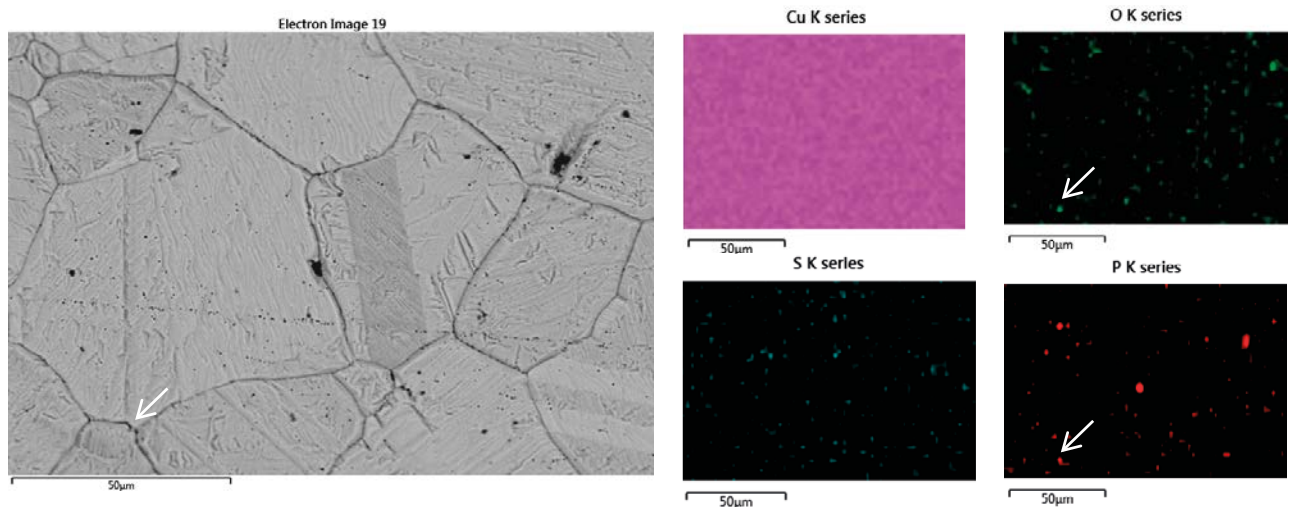


**Figure 4-6.** Oxidised high phosphorus OFP-Cu at 600 °C in  $N_2/H_2O/H_2$  environment. The surface of the sample is shown, as well as its corresponding Cu, O, S and P element maps. Chemical analysis by EDS at the location indicated by the arrow gives 51.2Cu–37.2O–6.6P, with other elements 1.9Si–1.8Ca.

An attempt was made to analyse the particulates on the surface of the sample with TEM based on FIB sample preparation. Small samples were cut out, but the particles had low adhesion to the metallic substrate and easily fell off. However, tiny particulates were found approximately 1  $\mu\text{m}$  beneath the surface and have been analysed as shown in Figure 4-7. Two particulates in a grain boundary, approximately 200 nm in size, are shown. Element maps, evaluated by EDS, are shown as well. The analysed specimen is thicker than the particle, and a mixed spectrum of particle and matrix is therefore analysed. It can be seen that the particulates are rich on oxygen and phosphorus, but low on copper. Some minor content of sulphur is measured as well. EDS analysis on the lower particle yield 72Cu–18.2O–9.3P–0.8S, in atomic percent.

The crystalline structures of copper matrix plus phosphorus rich oxide were evaluated using electron diffraction in TEM. The diffraction patterns are shown in Figure 4-8. The strongest pattern is from the copper matrix, and the faint pattern from the phosphorus rich particle. The faint diffraction pattern corresponds to inter-planar spacing 4.2  $\text{\AA}$ , 2.9  $\text{\AA}$ , 2.04  $\text{\AA}$ , and 1.8  $\text{\AA}$ . This diffraction pattern has been compared with the reported diffraction patterns for several different compounds. The most stable compounds belonging to the Cu–O–P system plus copper sulphide  $\text{Cu}_2\text{S}$  and copper oxide  $\text{Cu}_2\text{O}$  were chosen in this evaluation (Magnusson and Frisk 2013, 2014). This comparison is shown in Table 4-1, based on data taken from diffraction database (PDF-4+ 2015). It can be seen that reported diffraction data for  $\text{Cu}_3(\text{PO}_4)_2$  phosphate is the only phase that can explain all the measured reflections.

**Table 4-1. The table summarises the evaluate compounds and if they will give a reflection at the measured inter-planar spacings  $d_{hkl}$ . Data is taken from PDF-4+ diffraction database (PDF-4+ 2015). In the evaluation 30 % relative intensity was considered as a limit, and  $\pm 0.1 \text{ \AA}$  was allowed.**

Compound	Space group	Reflection at $d_{hkl}$				PDF-4+ id, reference
		4.2 $\text{\AA}$	2.9 $\text{\AA}$	2.04 $\text{\AA}$	1.8 $\text{\AA}$	
$\text{Cu}_3(\text{PO}_4)_2$	P-1	x	x	x	x	00-055-0486, Bamberger et al. 1997
$\alpha\text{-Cu}_2\text{P}_2\text{O}_7$	C2/c		x			04-007-7311, Effenberger 1990
$\beta\text{-Cu}_2\text{P}_2\text{O}_7$	C2/m		x			01-074-1614, Robertson and Calvo 1968
$\alpha\text{-P}_2\text{O}_5$	Fdd2	x	x			01-071-6182
$\alpha'\text{-P}_2\text{O}_5$	Pnma		x			04-007-0891
$\text{Cu}_2\text{O}$	Pn-3m			x		01-078-2076
$\text{Cu}_2\text{S}$	R-3m		x	x		00-026-0476
$\text{Cu}_2\text{S}$	Fm-3m		x	x		01-070-9132

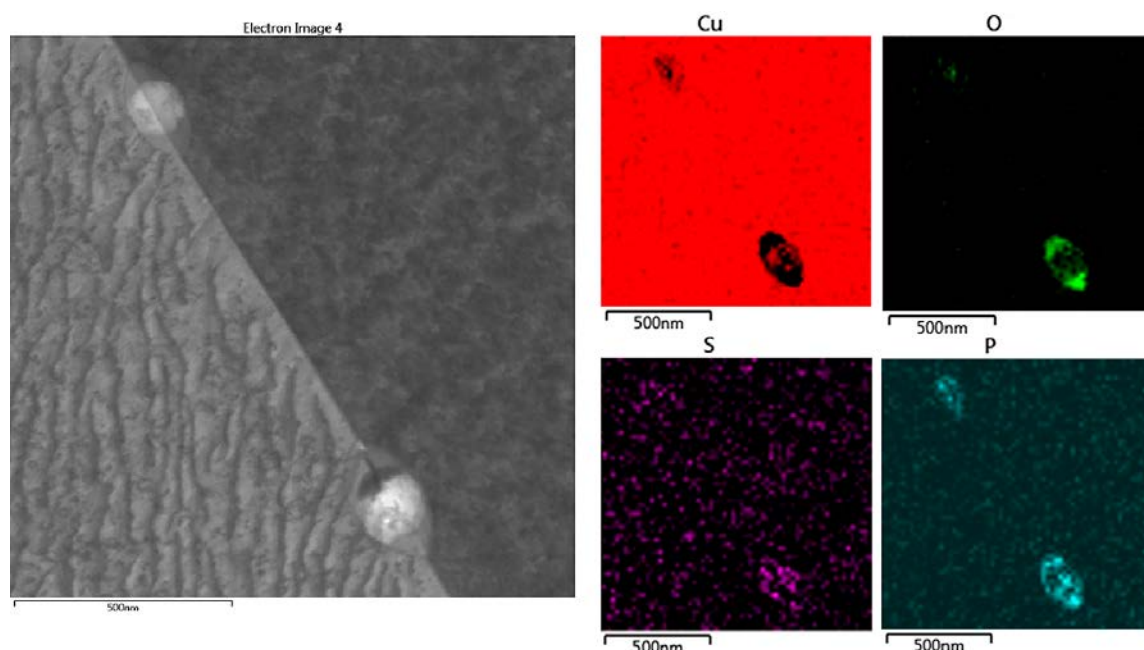


**Figure 4-7. TEM image of oxidised high phosphorus OFP-Cu at 600 °C in  $\text{N}_2/\text{H}_2\text{O}/\text{H}_2$ , with corresponding element maps determined with EDS analysis.**

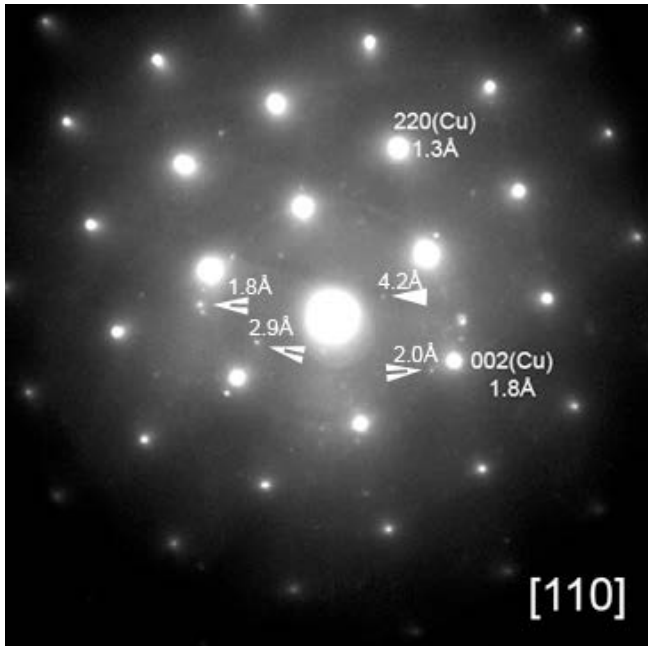


*Figure 4-8. Diffraction pattern of copper matrix with [110] zone-axis plus particle.*





# 5 Discussion

## 5.1 Surface copper oxides

The results from the oxidation made in this work will now be compared with calculations, and other observations found in the literature. The calculated stability of copper oxides  $\text{Cu}_2\text{O}$  and  $\text{CuO}$  relative metallic copper is presented in Figure 5-1, in similarity to Figure 3-1 but only showing the copper oxides. Oxidation experiments made in air gives a high oxygen activity close to unity. At this condition the outer oxide in contact with the atmosphere is  $\text{CuO}$ . This has been reported by Wang and Cho (2009) on 99.99 % Cu oxidised in air at 500–700 °C, and by Liang et al. (2012) on oxidised 4N6 copper at 700–900 °C. The surface oxides in these studies were  $\text{CuO}$ , but below this oxide layer  $\text{Cu}_2\text{O}$  is typically found in contact with the metallic copper. This has been found in other studies as well, as summarised in the review by Zhu et al. (2006). These findings are in agreement with the thermodynamics that  $\text{CuO}$  is present at the highest oxygen activities and  $\text{Cu}_2\text{O}$  can be stable to lower oxygen activities, as shown in Figure 5-1.

An industrial method to produce  $\text{Cu}_2\text{O}$  is by thermal oxidation in air or oxygen at high temperatures. A temperature above 1000 °C is needed to produce mainly  $\text{Cu}_2\text{O}$  and not  $\text{CuO}$  (Musa et al. 1998). An oxygen rich gas corresponds to an oxygen activity close to one. Above 1000 °C and at oxygen activity close to one the  $\text{Cu}_2\text{O}$  oxide is calculated stable. An alternative method to produce  $\text{Cu}_2\text{O}$  has been suggested recently by Liang et al. (2012). This method is to oxidise copper in water vapour plus inert gas. Liang et al. (2012) oxidised in water vapour with nitrogen as carrier gas. The exact mixture of the gas was not stated, and it is here assumed as 10 % water vapour. The  $\text{Cu}_2\text{O}$  phase region exists in several orders of magnitude in oxygen activity, and changing the water vapour content in nitrogen gas will have little influence on the results. Similar experiments have been made for Htay et al. (2014) on 99.999 % copper oxidised at 450–580 °C. They found  $\text{Cu}_2\text{O}$  as only oxides on all samples. Both these studies are in agreement with the experiment made in the present work where nitrogen plus water vapour was used to oxidise copper at 580 °C. Reported oxide layer thickness is in agreement with the oxidation made in this work. Liang et al. reported 5  $\mu\text{m}$  oxide layer after 2 hours at 700 °C, and Htay et al. reported 0.5  $\mu\text{m}$  after 0.5 hour at 530 °C. In this study, in average 3  $\mu\text{m}$  oxide layer was achieved after 24 hours oxidation at 580 °C.

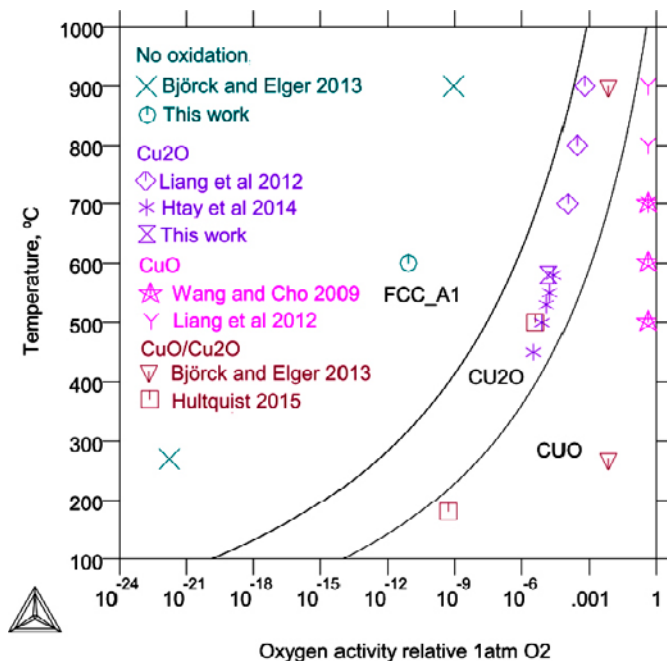


**Figure 5-1.** Calculated stability of copper oxides according to thermodynamic description of Cu–O system taken from Magnusson and Frisk (2013). Experimental data is taken from different references. The oxygen activity of the gas mixtures are calculated using the SSUB3 database (Thermo-Calc 2015).

The observed oxide thickness agrees with other studies but it should be mentioned that a 3  $\mu\text{m}$  oxide layer corresponds to more consumed oxygen than a mass-balance calculation yields based on 24 hours exposure in the used  $\text{N}_2/\text{H}_2\text{O}$  atmosphere. One explanation for this could be that oxidation occurs by the release of more oxygen through the water reaction, according to  $\text{H}_2\text{O} \rightleftharpoons \text{H}_2 + 0.5\text{O}_2$ . This reaction can occur until the partial pressure oxygen has fallen to the FCC/ $\text{Cu}_2\text{O}$  phase boundary, as illustrated in Figure 5-1. This reaction will supply more oxygen to the atmosphere, but according to the thermodynamics this reaction cannot alone supply sufficient amount of oxygen in order to oxidise 3  $\mu\text{m}$  of copper. Another explanation is that the instrumental grade of nitrogen (99.999 %) used in oxidation contained traces of oxygen or other oxidising gases such as  $\text{CO}_2$  that promotes oxidation. This could explain why the kinetics of  $\text{Cu}_2\text{O}$  oxidation occurred quicker than expected, and the oxidising partial pressure for the  $\text{N}_2/\text{H}_2\text{O}$  experiment could have been higher than stated in Table 3-1. Nevertheless, the oxidation made in this work produced a  $\text{Cu}_2\text{O}$  oxide layer with phosphorus rich oxides in it. This finding is in agreement with the thermodynamic evaluation that phosphorus should form its own oxides.

Some studies have been made where copper material was exposed to reducing atmospheres. A reducing atmosphere is here defined as an atmosphere where the hydrogen to oxygen atomic relation exceeds the relation of water 2:1. When hydrogen is in surplus, the available oxygen will be consumed by hydrogen and the oxygen partial pressure will rapidly fall. Björck and Elger (2013) oxidised OFP-copper in  $\text{Ar}+1.8\%\text{H}_2+0.1\%\text{O}_2$  at both 270 °C and 900 °C. These materials did not show any mass gain. This is in agreement with the oxidation in  $\text{N}_2/\text{H}_2\text{O}/\text{H}_2$  atmosphere made in this work, which did not show a dense copper oxide layer. All these findings are in agreement with calculations that indicate that the surface should remain as metallic copper.

Finally some further experiments are also given as reference, where oxidation has clearly occurred but the type of surface oxide was not characterised. Björck and Elger (2013) also oxidised OFP-copper in  $\text{Ar} + 100 \text{ ppm O}_2$  atmosphere. The oxidised material showed a significant mass gain. According to the calculations the surface oxide should have been  $\text{Cu}_2\text{O}$ . Additional experiments have been made by Hultquist (2015), who oxidised OFP-copper for 120 hours in 10 mbar water vapour at both 180 and 500 °C. These experiments were made in a closed system, in contrast to the other references given in Figure 5-1. In a closed system equilibrium will eventually be reached between the oxidising atmosphere and the copper material. The copper material will be oxidised and the free oxygen in the atmosphere will be consumed. The 10 mbar water vapour pressure at 500 °C is similar to the oxidising in  $\text{N}_2/\text{H}_2\text{O}$  atmosphere made in this work, and similar to the oxidation made by Htay et al. (2014). In both these works the surface oxide has been verified to be  $\text{Cu}_2\text{O}$ , which is in agreement with calculations. The 10 mbar water vapour atmosphere at 180 °C is predicted to be more oxidising and  $\text{CuO}$  is predicted as the outer oxide.

## 5.2 Phosphorus rich oxides

Phosphorus rich oxide was found in the oxidised samples. In the case of higher oxidising potential using  $\text{N}_2/\text{H}_2\text{O}$  atmosphere these phosphorus oxides were present in the  $\text{Cu}_2\text{O}$  oxide scale. When oxidised at more reducing conditions, in  $\text{N}_2/\text{H}_2\text{O}/\text{H}_2$ , the phosphorus rich oxides were present on the metallic copper surface without the presence of any copper oxides. By oxidising at this condition it was experimentally shown that phosphorus rich oxides are more stable than copper oxides. These experimental results verify the high affinity between phosphorus and oxygen. This has been predicted by the thermodynamic evaluation of the  $\text{Cu-H-O-S-P}$  system, but not previously shown by experiments. Quite few observations of oxides in OFP-copper exist in literature, and these are normally limited to welded materials.

Chemical analysis of the phosphorus rich oxides was made with both SEM and TEM using EDS detectors. A complication was that the oxides were often quite small and chemical analysis gave a mixed spectrum of oxide plus substrate. For oxidation in  $\text{N}_2/\text{H}_2\text{O}/\text{H}_2$  environment the substrate was metallic copper. The chemical analysis indicated a phosphorus rich oxide and up to 9 at% phosphorus was measured with TEM/EDS, as shown in Figure 4-7. For oxidation in  $\text{N}_2/\text{H}_2\text{O}$  environment the phosphorus rich oxide was located in the copper oxide scale. SEM/EDS measurements

on phosphorus rich oxide plus copper oxide showed an increase in phosphorus and oxygen contents compared to copper oxide alone, as shown in Figure 4-4. These results indicate the presence of a copper phosphate, however, the mixed spectrums makes it difficult to verify the type of phosphate.

In order to verify the type of phosphate electron diffraction was made. The diffraction results of phosphorus rich oxide in a copper grain boundary gave two distinct diffraction patterns, as shown in Figure 4-8. The strongest pattern belonged to the copper metal and the additional pattern showed a good agreement to reported data for the  $\text{Cu}_3(\text{PO}_4)_2$  copper phosphate. This finding is in agreement with thermodynamic calculations for this temperature and oxygen activity, as shown in Figure 3-1.

Few observations of phosphates in commercial copper grades are found in the literature. An obvious limitation in OFP-copper is the low oxygen content in the material, which is typically a few ppm. This will lead to a very low phase fraction of oxides. Another limitation is that in OFP-copper more than 99.99 % of all atoms are copper and if oxygen is present it is possible that metastable copper oxide might form first. In this work OFP-copper was saturated with oxygen, by oxidising in  $\text{N}_2/\text{H}_2\text{O}/\text{H}_2$  at 600 °C, in order to raise the phase fraction of phosphates. A copper material with 100 ppm phosphorus then yields approximately 500 ppm oxygen. This is much higher than normal canister OFP-copper, which is less than 5 ppm oxygen. It will be a difficult task to find where oxygen is located in normal OFP-copper grades due to the low oxygen content. It was shown in a previous work that phosphates are stable from solidus down to room temperature (Magnusson and Frisk 2013). This could explain why phosphates should be the oxygen compound in phosphorus alloyed oxygen-free copper, although this remains to be verified.



## 6 Conclusions

It has been validated in this work that the stability of copper oxides is accurately described by the thermodynamic description being used. Some findings regarding surface copper oxides:

- Oxidising copper in air at temperatures up to 1 000 °C will produce CuO as an outer oxide.
- Oxidising copper in water vapour with inert gas above approximately 300 °C, or in air above 1 000 °C, will produce Cu<sub>2</sub>O as the only copper rich surface oxide.
- Oxidising copper in reducing atmospheres (defined as H:O relation above 2:1) will lead to very low oxygen activities. At these conditions no copper oxides are stable.

The presence of phosphorus-rich oxides in OFP-copper has been validated in this work. Some findings for the phosphorus rich oxides:

- Phosphorus rich oxides were observed with both SEM and TEM. The oxides are small, less than 200 nm in size when oxidised 24 h at 580–600 °C.
- EDS measurements on these oxides give an increasing phosphorus content and oxygen content but falling copper content, compared to the copper oxide Cu<sub>2</sub>O. This is in agreement with typical copper phosphates like Cu<sub>2</sub>P<sub>2</sub>O<sub>7</sub> and Cu<sub>3</sub>(PO<sub>4</sub>)<sub>2</sub>.
- Electron diffraction results show that the phosphorus rich compound is most likely Cu<sub>3</sub>(PO<sub>4</sub>)<sub>2</sub>, which is the equilibrium phosphate at these oxidising conditions.
- It has been experimentally shown in this work how copper phosphates can be stable to lower partial pressure oxygen than copper oxides. This verifies that copper phosphates have a higher stability than copper oxides at low oxygen activities.



## References

SKB's (Svensk Kärnbränslehantering AB) publications can be found at [www.skb.com/publications](http://www.skb.com/publications). SKBdoc-documents will be submitted upon request to [document@skb.se](mailto:document@skb.se).

**Andersson H, Seitisleam F, Sandström R, 1999.** Influence of phosphorus and sulphur as well as grain size on creep in pure copper. SKB TR-99-39, Svensk Kärnbränslehantering AB.

**Ball M C, 1968.** Phase-equilibrium relationships in the systems  $\text{CuO-P}_2\text{O}_5$  and  $\text{Cu}_2\text{O-P}_2\text{O}_5$ . Journal of the Chemical Society A 1968, 1113–1115.

**Bamberger C E, Specht E D, Anovitz L M, 1997.** Crystalline copper phosphates: synthesis and thermal stability. Journal of the American Ceramic Society 80, 3133–3138.

**Björck M, Elger R, 2013.** Oxidation kinetics of copper at reduced oxygen partial pressures. SKBdoc 1410172 ver 1.0, Svensk Kärnbränslehantering AB.

**Effenberger H, 1990.** Structural refinement of low-temperature copper (II) pyrophosphate. Acta Crystallographica C46, 691–692.

**Htay M T, Masahiko O, Yoshizawa R, Hashimoto Y, Ito K, 2014.** Synthesis of a cuprite thin film by oxidation of a Cu metal precursor utilizing ultrasonically generated water vapour. Thin Solid Films 556, 211–215.

**Hultquist G, 2015.** Why copper may be able to corrode in pure water. Corrosion Science 93, 327–329.

**Liang J, Kishi N, Soga T, Jimbo T, Ahmed M, 2012.** Thin cuprous oxide films prepared by thermal oxidation of copper foils with water vapour. Thin Solid Films 520, 2679–2682.

**Lukas H L, Fries S G, Sundman B, 2007.** Computational thermodynamics: the Calphad method. Cambridge: Cambridge University Press.

**Magnusson H, Frisk K, 2013.** Thermodynamic evaluation of Cu–H–O–S–P system. Phase stabilities and solubilities for OFP-copper. SKB TR-13-11, Svensk Kärnbränslehantering AB.

**Magnusson H, Frisk K, 2014.** Thermodynamic evaluation of the copper-rich part of the Cu–H–O–S–P system at low temperatures. Calphad 47, 148–160.

**Magnusson H, Bergman O, Frisk K, 2013.** An experimental and computational technique suitable for characterisation of oxides. In Proceedings of International Powder Metallurgy Congress and Exhibition, Euro PM 2013, Gothenburg, Sweden, 15–18 September 2013.

**Musa A O, Akomolafe T, Carter M J, 1998.** Production of cuprous oxide, a solar cell material, by thermal oxidation and a study of its physical and electrical properties. Solar Energy Materials and Solar Cells 51, 305–316.

**PDF-4+, 2015.** The powder diffraction file. Newtown Square, PA: International Centre for Diffraction Data.

**Robertson B E, Calvo C, 1968.** Crystal structure of  $\beta\text{-Cu}_2\text{P}_2\text{O}_7$ . Canadian Journal of Chemistry 46, 605–612.

**Saunders N, Miodownik A P, 1998.** Calphad: calculation of phase diagrams: a comprehensive guide. Oxford: Elsevier.

**Savolainen K, 2012.** Friction stir welding of copper and microstructure and properties of the welds. PhD thesis. Aalto University, Helsinki, Finland.

**SKB, 2010.** Design, production and initial state of the canister. SKB TR-10-14, Svensk Kärnbränslehantering AB.

**Smart J S, Smith A A, 1946.** Effect of phosphorus, arsenic, sulphur, and selenium on some properties of high-purity copper. Transactions of the American Institute of Mining, Metallurgical and Petroleum Engineers 166, 144–155.

**SSUB3, 2015.** SGTE Substance Database SSUB3 by Scientific Group Thermodata Europe. Stockholm: Thermo-Calc Software AB.

**Thermo-Calc, 2015.** Thermo-Calc version 4.1. Stockholm: Thermo-Calc AB.

**Wang J-P, Cho W D, 2009.** Oxidation behaviour of pure copper in oxygen and/or water vapour at intermediate temperature. ISIJ international 49, 1926–1931.

**Zhu Y, Mimura K, Lim J W, Isshiki M, Jiang Q, 2006.** Brief review of oxidation kinetics of copper at 350 °C to 1050 °C. Metallurgical and Materials Transactions 37A, 1231–1237.



